Journal of Alzheimer's Disease 101 (2024) 309–320
DOI 10.3233/JAD-240484
IOS Press

First Biodistribution Study of [^{68}Ga]Ga-NOTA-Insulin Following Intranasal Administration in Adult Vervet Monkeys

Kiran Kumar Solingapuram Sai[a,1], Jennifer M. Erichsen[b,1], Krishna K. Gollapelli[a], Ivan Krizan[a], Mack Miller[a], Avinash Bansode[a], Mathew J. Jorgensen[c], Thomas Register[c], Charles Cazzola[d], Reenal Gandhi[e], Julie Suman[e] and Suzanne Craft[b,*]
[a]*Department of Radiology, Wake Forest School of Medicine, Winston-Salem, NC, USA*
[b]*Department of Internal Medicine, Division of Gerontology and Geriatric Medicine, Wake Forest School of Medicine, Winston-Salem, NC, USA*
[c]*Department of Pathology, Division of Comparative Medicine, Wake Forest School of Medicine, Winston-Salem, NC, USA*
[d]*Aptar Pharma, Le Vaudreuil, France*
[e]*Aptar Pharmaceuticals, Congers, NY, USA*

Accepted 20 June 2024

Abstract.
Background: Intranasal insulin (INI) is being explored as a treatment for Alzheimer's disease (AD). Improved memory, functional ability, and cerebrospinal fluid (CSF) AD biomarker profiles have been observed following INI administration. However, the method of intranasal delivery may significantly affect outcomes.
Objective: To show reliable delivery of insulin to the brain using the Aptar Cartridge Pump System (CPS) intranasal delivery system.
Methods: To visualize INI biodistribution, we developed a novel PET radiotracer, Gallium 68-radiolabeled (NOTA-conjugated) insulin, [^{68}Ga]Ga-NOTA-insulin. We used the Aptar CPS to administer [^{68}Ga]Ga-NOTA-insulin to anesthetized healthy adult vervet monkeys and measured brain regional activity and whole-body dosimetry following PET/CT scans.
Results: We observed brain penetration of [^{68}Ga]Ga-NOTA-insulin following intranasal administration with the Aptar CPS. Radioactive uptake was seen in multiple regions, including the amygdala, putamen, hypothalamus, hippocampus, and choroid plexus. A safety profile and whole-body dosimetry were also established in a second cohort of vervets. Safety was confirmed: vitals remained stable, blood glucose levels were unchanged, and no organ was exposed to more than 2.5 mSv of radioactivity. Extrapolations from vervet organ distribution allowed for estimation of the [^{68}Ga]Ga-NOTA-insulin absorbed dose in humans, and the maximum dose of [^{68}Ga]Ga-NOTA-insulin that can be safely administered to humans was determined to be 185 MBq.
Conclusions: The use of [^{68}Ga]Ga-NOTA-insulin as a PET radiotracer is safe and effective for observing brain uptake in vervet monkeys. Further, the Aptar CPS successfully targets [^{68}Ga]Ga-NOTA-insulin to the brain. The data will be essential in guiding future studies of intranasal [^{68}Ga]Ga-NOTA-insulin administration in humans.

Keywords: Alzheimer's disease, insulin, intranasal administration, primates

[1]These authors contributed equally to this work.

*Correspondence to: Suzanne Craft, Department of Internal Medicine, Division of Gerontology and Geriatric Medicine, Wake Forest School of Medicine, One Medical Center Boulevard Winston-Salem, NC 27157, USA. Tel.: +1 336 713 8832; E-mail: suzcraft@wakehealth.edu.

INTRODUCTION

Although the disease-modifying anti-amyloid monoclonal antibodies have shown promise in clearing amyloid plaques from the brain and slowing the progression of Alzheimer's disease (AD), these therapies have been only modestly efficacious in improving symptoms.[1,2] Globally, investigators are still searching for a more effective AD treatment as the societal burden of this neurodegenerative disease continues to grow. Insulin is currently being explored as a therapeutic agent in several preclinical and clinical settings, as it has been suggested that the insulin signaling pathway is dysregulated in patients with AD.[3] Restoration of this pathway in the brain via insulin treatment may overcome insulin resistance and, ultimately, improve cognition and AD pathologic processes.[4]

Insulin can be targeted directly to the central nervous system (CNS) via the intranasal (nose-to-brain) delivery pathway. This route bypasses the periphery, avoiding hypoglycemia and other adverse systemic effects.[5] Following intranasal administration, insulin travels from the nasal mucosa to the CNS via extracellular bulk flow along the olfactory and trigeminal nerves.[6] It then diffuses into the subarachnoid space and from there, into the cerebrovasculature, where it gets rapidly dispersed throughout the brain. There are over 100 ongoing and/or completed clinical trials investigating the effects of intranasal insulin (INI); several of these are exploring the effects in individuals with varying degrees of cognitive impairment. These studies have revealed effects including enhanced memory, augmented functional ability, improved cerebrospinal fluid (CSF) AD biomarker profiles, and preserved brain volume. In our recent 18-month phase II clinical trial, INI improved cerebral glucose utilization, AD CSF biomarker profiles, white matter hyperintensity volume progression, and cognition in adults with mild cognitive impairment (MCI) or preclinical AD; however, these effects were only observed in a cohort of participants that used one of the two utilized delivery devices.[7] This discrepancy raised the possibility that the failure of the one device may have been due to its method of delivery. Before proceeding with future INI clinical trials that further explore therapeutic efficacy, it is imperative to identify an intranasal delivery device that reliably and effectively delivers insulin to the brain.

Positron emission tomography (PET) imaging is a sensitive imaging modality that can be used to study biochemical functions in real time. Further, PET imaging is becoming a standard tool for assessing AD pathophysiology, as this technique accurately captures the functional changes in biomarkers and is therefore useful for AD diagnosis, stratification, and tracking of therapeutic progress. In this study, we used PET imaging to examine the distribution of a PET radiotracer, Gallium 68-radiolabeled insulin ([^{68}Ga]Ga-NOTA-insulin) following intranasal administration. This is the first study to use this radiotracer to label insulin. We utilized an intranasal delivery device that was developed and extensively tested by Aptar Pharma[8], a company specializing in drug delivery solutions. The Aptar Cartridge Pump System (CPS) is a multidose delivery system having an integrated multilayer filter membrane with a pore size of 0.2 micrometers, which filters the airflow back into the bottle/container and insulin is delivered through a nozzle with a spring-loaded tip seal.

A safety and efficacy profile for [^{68}Ga]Ga-NOTA-insulin in wild-type and AD mice has already been established.[9] However, no insulin-based PET studies in non-human primates (NHPs) have been reported. NHPs form an excellent model for translational imaging studies as their metabolism, anatomy, and physiology are similar to those of humans.[10,11] Additionally, no dosimetry studies have heretofore been established. Dosimetry studies are critical in clinical translational studies as they provide an estimation of exposed radiation to major organs after a single dose administration of the PET radiotracer. Therefore, to evaluate the clinical utility of [^{68}Ga]Ga-NOTA-insulin and verify intranasal delivery via the pump system, we studied the whole-body biodistribution and calculated the absorbed radiation exposure for dosimetry analysis in eight healthy adult vervet monkeys ($n = 4$/sex). This study allowed for the visualization of insulin biodistribution in the brain ($n = 8$) following intranasal administration, along with whole body dosimetry ($n = 4$/sex). The data will be essential in guiding future studies of intranasal [^{68}Ga]Ga-NOTA-insulin administration in humans.

MATERIALS AND METHODS

Animal preparation

All animal housing and handling and all experimental procedures were performed in accordance with the National Institutes of Health Guide for the Care and Use of Laboratory Animals[12] and approved by the Wake Forest University School of Medicine

Table 1
NHP characteristics

Type of scan	Sex	Age (y)	Weight (kg)
Brain	Female	14.7	4.1
Brain	Female	17.5	7.1
Brain	Male	8.2	8.4
Brain	Male	9.7	7.8
Brain	Male	10.5	6.2
Brain	Male	10.6	6.8
Brain	Male	10.9	7.2
Brain	Male	11.3	6.7
	Mean	**11.7**	**6.8**
Whole body	Female	8.1	4.5
Whole body	Female	8.1	5.4
Whole body	Female	11.3	6.2
Whole body	Female	12.2	4.5
Whole body	Male	11.3	6.2
Whole body	Male	11.6	6.7
Whole body	Male	12.0	6.6
Whole body	Male	13.1	6.6
	Mean	**11.0**	**5.8**

Animal Care and Use Committee (ACUC). Environmental enrichment of all animals followed ACUC's NHP Environmental Enrichment Plan. Additionally, the research presented in this manuscript was performed in accordance with the American Society of Primatologists Principles for the Ethical Treatment of NHPs. Subjects for this study were sixteen adult captive vervet monkeys (Table 1) housed as part of the Vervet Research Colony (VRC) at the Wake Forest School of Medicine; $n = 8$ underwent 60-min PET scans to measure specific brain regional activity of the radiotracer, and $n = 8$ had 180-min whole body dosimetry scans. Subjects were housed at the VRC in matrilineal social groups that resemble vervet social groups in the wild. Animals were housed with indoor-outdoor access and provisioned daily with commercial monkey chow (Purina Monkey Chow, LabDiet 5038) along with supplementary fresh fruits and vegetables. Vervet monkeys were chosen for this study as they are relatively easy to handle, less expensive than rhesus macaques,[13] and, similar to humans, naturally develop several risk factors for AD including obesity and prediabetes.[14] Additionally, Wake Forest University and the Jorgensen laboratory have supporting physiologic data for vervets. Finally, vervet monkeys have previously been shown to have a nasal cavity anatomically similar to humans, which is especially critical for a study such as this.

Animals were fasted prior to any imaging; depending on the start time of the scan, they were either clean fasted for 12 h or morning fasted for 6 h. Approximately 2 h before the scan was to start, a VRC laboratory technician sedated each animal with ketamine (15 mg/kg; intramuscular) and administered atropine (0.03 mg/kg; intramuscular). The animal was then weighed, vitals were obtained, and a blood glucose measurement was recorded using an AccuCHEK glucometer. The animal was then transported to the PET/CT imaging suite, where the anesthesia technician began mask induction with isoflurane (2–3%) and provided heat support and monitoring equipment. Two intravenous catheters were placed into each hind limb saphenous vein. The animal was then positioned in a reclined seated position and wrapped in a warm blanket until the radiotracer was ready to be administered via intranasal route.

Synthesis of NOTA-insulin

In the pursuit of developing a PET probe utilizing insulin, we employed 2-S-(4-isothiocyanatobenzyl)-1,4,7-triazacyclonone-1,4,7-triacetic acid (p-SCN-Bn-NOTA) to link with the primary amine of the lysine residue in insulin chain B. Specifically, in a clean and dry glass vial equipped with a magnetic stir bar, NOTA-NCS (3.2 mg, 0.0057 mmol, 2.46 equiv) obtained from Macrocyclics, Plano, TX, was accurately weighed, dissolved in molecular biology-grade water (0.4 mL) (Sigma-Aldrich, St. Louis, MO). To the reaction vessel, human insulin (13.5 mg, 0.0023 mmol, 1.00 eq, Sigma Aldrich, St. Louis) was added and the pH of reaction mixture was adjusted to 6.3–6.5 by 0.1 N Na_2CO_3 (78 μL), and the reaction was stirred at room temperature for 5 h. Crude product was subsequently stored at –20°C.

Purification of NOTA-insulin by size exclusion chromatography

Purification of NOTA-Insulin via Size Exclusion Chromatography involved preparing a PD-10 column (Cytiva, Global Life Sciences, USA) following the manufacturer's guidelines.[9] The column was equilibrated with 4 column volumes of 1.0 M NaOAc buffer (pH = 6.5) and subsequently, the crude NOTA-insulin was transferred from the reaction vessel to the column. The reaction vessel was then washed with 1.0 mL of 1.0 M NaOAc buffer (pH = 6.5), and the wash was loaded onto the column, discarding

the flow through. Elution of NOTA-insulin occurred in 6 × 1 mL fractions using 1.0 M sodium acetate buffer (pH = 6.5). Analytical high-performance liquid chromatography (HPLC) of the purified NOTA-insulin was conducted on a Luna 5 μm C18 100 Å LC Column (250 × 4.6 mm) with a UV detector wavelength of 214 nm. The flow rate was set at 0.5 mL/min, employing a gradient mobile phase (Eluent A: 0.1% TFA in acetonitrile; Eluent B: 0.1% TFA in water): 25% A at 0 min, followed by 30% A at 5 min, and 32.2% A from 10 to 90 min. The obtained fractions were scrutinized for chemical purity. Confirmatory analysis using HPLC indicated a mono-NOTA-insulin percentage exceeding 90%, surpassing unreacted insulin, di-NOTA-insulin, and tri-NOTA-insulin. Maintaining the reaction pH close to 6.3 emerged as a critical factor, substantiated by HPLC analysis of PD-10 purified fractions. This demonstrated that mono-NOTA-insulin consistently exceeded unreacted insulin, di-NOTA-insulin, and tri-NOTA-insulin.

Radiochemical synthesis of [^{68}Ga]Ga-NOTA-insulin]

The synthesis of [^{68}Ga]Ga-NOTA-insulin involved adding 1.0 mL of [^{68}Ga]$GaCl_3$ (obtained from Cardinal Health, Greensboro, NC) to a clean glass vial. Subsequently, 70 μL of 3.0 M sodium acetate buffer (pH = 8.5) was introduced to adjust the pH to 4.4–4.7. The addition of 100 μL of mono-NOTA-insulin to the mixture was followed by stirring at room temperature for 5 min (Fig. 1). The final pH was maintained at 6.1–6.5 with 180 μL of 3 M NaOAc buffer (pH = 8.5), and the resulting product underwent filtration through a Millex-GV 0.22 μm sterile filter unit (Merck, Kenilworth, NJ).

Radio-iTLC

Radio-iTLC was conducted with iTLC-SG paper (Agilent Technologies, Santa Clara, CA), which was developed in 0.1 M sodium citrate solution (pH = 7) and examined using a radio-iTLC scanner (Eckert & Ziegler, Valencia, CA). The Rf values for [^{68}Ga]Ga-NOTA-insulin and free [^{68}Ga] were observed at 0.0–0.2 and 0.8–1.0, respectively (Fig. 2).

Stability analysis

The *in vitro* stability of [^{68}Ga]Ga-NOTA-insulin was assessed at room temperature at 0, 30, 60, 90, 120, 180, 240, and 300 min post radiotracer production. Radio-iTLC was employed using ∼0.037 MBq of [^{68}Ga]Ga-NOTA-insulin (at each time-point) onto the TLC plate to examine the radiochemical purity. After confirming the stability of [^{68}Ga]Ga-NOTA-insulin, we performed the *in vivo* evaluation of [^{68}Ga]Ga-NOTA-insulin following intranasal administration in adult vervets.

Intranasal administration

First, blood (0.5–1.5 mL) was collected from a saphenous vein catheter using the "push-pull" method to flush the catheter 3 times with 5 mL saline; this served as the baseline blood collection. A baseline blood glucose measurement was taken from this sample using an AccuCHEK glucometer. The [^{68}Ga]Ga-NOTA-insulin was then administered intranasally via the pump system (Fig. 3) under light mask induction. Two puffs were delivered into each nostril, with 1 min between each of the four puffs. All animals received 30 ± 2 MBq of [^{68}Ga]Ga-NOTA-insulin (∼4.0–9.0 International Units (IU) of insulin). Immediately following the final radioactive puff, the animal was intubated with an endotracheal tube and positioned dorsally. Vervets were under anesthesia breathing circuit/ventilator with constant intravenous saline fluid support (1 drop/15 seconds). A low-resolution CT scan was performed for anatomical co-registration application, immediately followed by a PET scan. All the PET scans were initiated within 8 min of the final puff of insulin. Scan durations were as follows: 60-min brain scans and 180-min whole-body dosimetry scans. Anesthesia and record vitals were monitored throughout the duration of the scan. Blood samples (0.5–1.5 mL) were collected from alternating saphenous vein catheters at the following timepoints during the brain scans: 3, 10, 25, 30, and 60 min, and from these timepoints during the whole-body dosimetry scans: 5, 10, 15, 20, 30, 60, 90, 120, 150, 180 min. A blood glucose measurement was immediately taken from the samples at each of these timepoints. The collected blood was stored in heparinized 1.5 mL microcentrifuge tubes, which were inverted 8–10x to alleviate coagulation and placed on ice. The samples were then centrifuged at 2000xg for 10 min at 4°C. Plasma and buffy coat were aliquoted into 0.5mL polypropylene cryovials and stored at –80°C for further processing. Insulin and HbA_{1c} measurements were collected from these stored aliquots. Following completion of the scan, standard post-procedural monitoring occurred. The

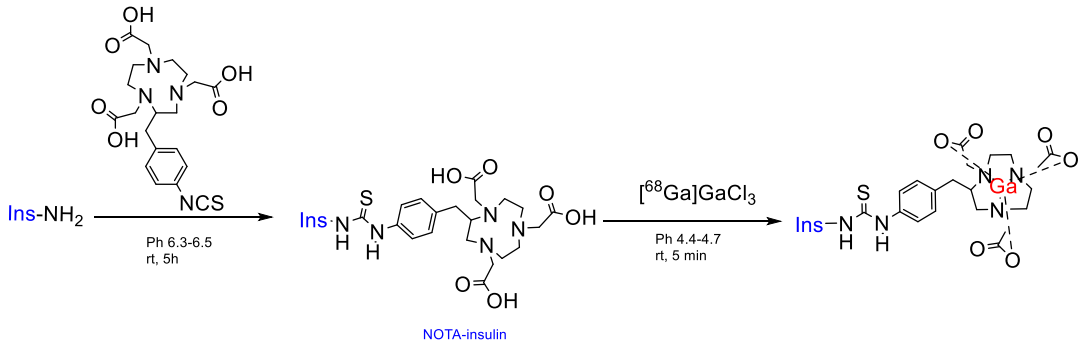

Fig. 1. Radiochemistry of [^{68}Ga]Ga-NOTA-insulin.

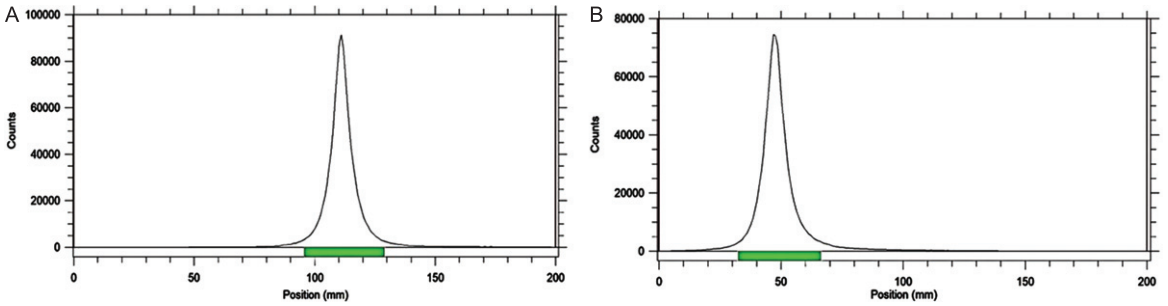

Fig. 2. Radio-iTLC chromatogram of [^{68}Ga]Ga-NOTA-insulin: A) Free [^{68}Ga]Cl_3, B) [^{68}Ga]Ga-NOTA-insulin with 99% radiochemical purity. Conditions: C18 TLC plates using 0.1 M sodium citrate solution (pH = 7) as mobile phase.

animals recovered in the PET/CT suite until they were at Stage 3/Consciousness and were then transported back to housing and all animals were monitored to ensure Stage 2 recovery.

Dosimetry

Four male and four female adult healthy vervet monkeys (8.1–13.1 y) underwent 180-min whole-body PET/CT acquisition using the GE Discovery MIDR PET/CT scanner, following intranasal administration of ~25–30 MBq of [^{68}Ga]Ga-NOTA-insulin using the pump system. PET images were acquired with 5-bed positions from head to pelvis regions and binned with 2.5 min per bed with 15 positions (totaling for 180 min). The five bed positions of each whole-body PET scan were assembled in a volume with 128×269 voxels, with a $2.6 \times 2.6 \times 2.6\,mm^3$ voxel size. A whole-body CT scan was obtained and reconstructed applying attenuation and scatter corrections. Three-dimensional volume of interests (VOIs) were identified using PMOD software (PMOD 4.304, (PMOD Technologies Ltd, Zurich, Switzerland;www.pmod.com)) on the transaxial or coronal slices of the PET frames, using NHP atlas and CT/MRI images on all the standard dosimetry organs (Table 3). To achieve a proper NHP-human dosimetry calculation with NHP PET acquisition data, the organ radioactivity values were corrected for recovery related to large VOIs that included the entire body for each frame,[15] as described earlier.[16] Thus, the residual activity value for each organ at every time point was scaled to the measured decay-corrected recovery for the individual frames. VOIs were then imported to Voxel Dosimetry (Voxel dosimetry 2.0) software and their associated effective absorbed dose was extrapolated using the primate tissue weighting factor. Using PMOD software, the time activity curve (TAC) and time-integrated activity coefficient (TIAC) for each organ were determined from the effective dose values, and the organ residence times were calculated by integration of the TIACs.[17]

Statistical analysis

Unpaired *t*-tests were used to probe for the effect of sex on tracer uptake in each brain region. Correlations and simple linear regression were also run between age and tracer uptake within each brain region. A one-

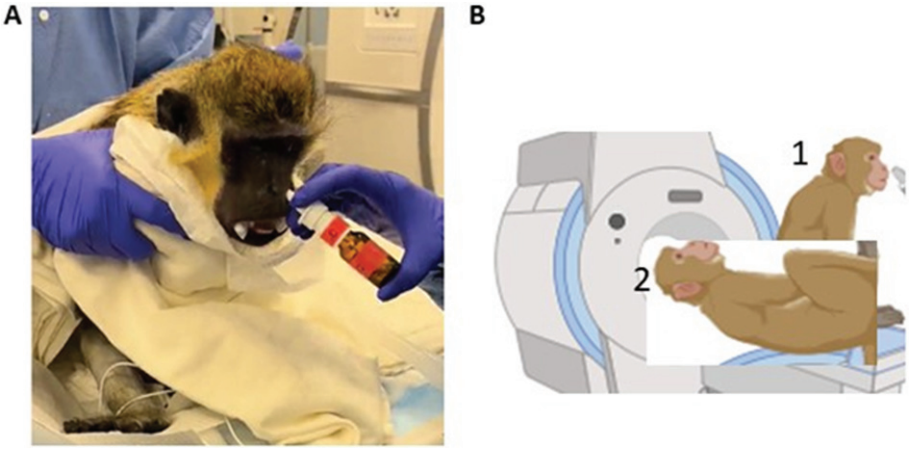

Fig. 3. A) Visual representation of the intranasal administration delivery procedure. B) Representative cartoon of animal positioning (1) during and (2) after intranasal administration.

way ANOVA was used to analyze changes in blood glucose levels over time.

RESULTS

Synthesis of [^{68}Ga]Ga-NOTA-insulin

As described in the Methods, human-grade insulin was chelated with NOTA and radiolabeled with [^{68}Ga] at room temperature to obtain [^{68}Ga]Ga-NOTA-insulin in high (>99%) radiochemical purity and molar activity (~106 GBq/μmol) decay corrected to end-of-synthesis.[18] Purity of the mono-NOTA insulin was > 90% for all the productions; specifically, the obtained fractions yielded 13.3 mg (92% chemical purity).

Specific brain regional activity of [^{68}Ga]Ga-NOTA-insulin

Eight adult vervet monkeys ($n = 6$ males; age range 8.2–17.5 years, mean 11.7 years) underwent a 60-min brain PET scan to measure specific brain regional activity of the radiotracer following intranasal administration. On average, the amygdala was the brain region that demonstrated the highest regional activity, with a mean PET standard uptake value (SUV) of 0.7456 ± 0.2814 g/ml (Fig. 4). This was followed by the putamen (0.5574 ± 0.2131 g/ml), choroid plexus (0.5089 ± 0.1650 g/ml), and hypothalamus (0.4760 ± 0.1990 g/ml). Brain regional activity did not differ according to sex or age in any of the examined regions. Representative PET-MR images are shown in Fig. 5.

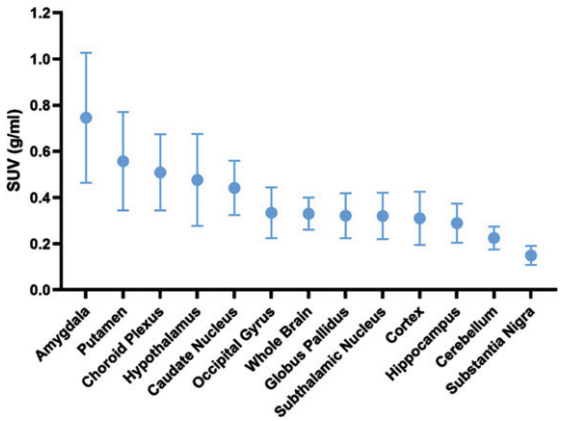

Fig. 4. PET brain regional uptake. Uptake was highest in the amygdala, putamen, and choroid plexus. SUV = standard uptake value, represented as mean uptake ± standard error of the mean (SEM).

Dosimetry

Eight healthy adult vervets ($n = 4$/sex; age range 8.1–13.1 years, mean 11.0 years) underwent 180-min whole body dosimetry PET scans following the intranasal administration of [^{68}Ga]Ga-NOTA-insulin. Brain uptake was highest between 20–60 min after intranasal administration, and negligible after 60 min (Fig. 6). No significant differences were seen between sexes or according to age with regard to uptake in any region. Slightly higher activity was observed in the nasal cavity and eyes in comparison to other organs (Fig. 7); this was expected as a result of the intranasal delivery method and supine position in the PET scanner. Overall, favorable whole body radioactivity values were observed. With all vervets,

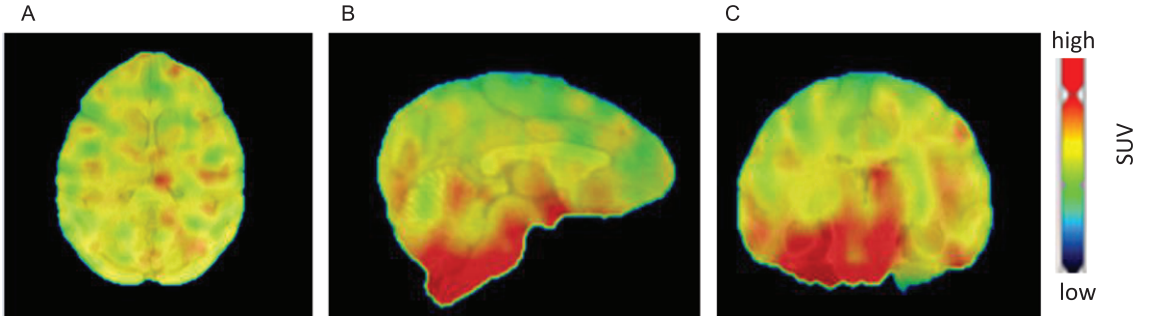

Fig. 5. Representative A) coronal, B) sagittal, and C) axial brain PET-MR coregistered images after intranasal administration of [^{68}Ga]Ga-NOTA-insulin. Highlighted PET (radioactive) uptake in the brain region clearly demonstrates the brain penetration of the radiotracer.

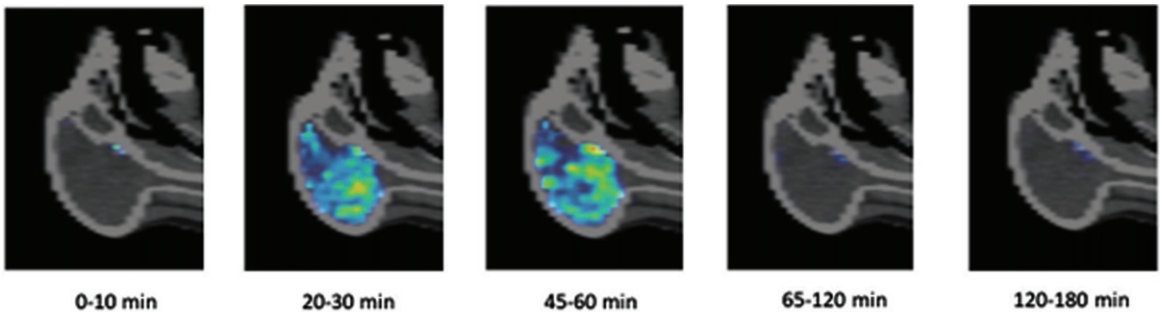

Fig. 6. Representative time-activity dosimetry PET/CT image of a vervet brain vervet following intranasal administration of [^{68}Ga]Ga-NOTA-insulin.

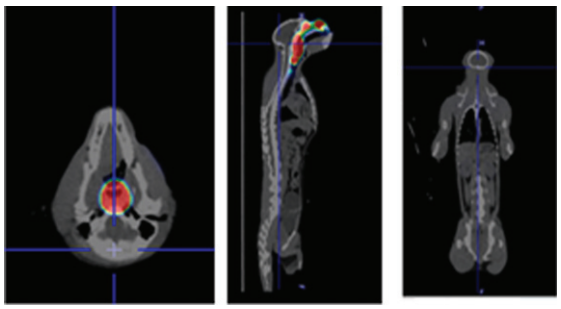

Fig. 7. Whole body dosimetry PET images. Representative whole-body PET/CT images of a vervet (axial, sagittal, and transverse views), after 3 h of intranasal administration of [^{68}Ga]Ga-NOTA-insulin.

vitals remained stable throughout the 3 h scanning period and 24 h recovery, establishing a high safety profile.

Blood glucose measurements

Blood glucose was measured at baseline and monitored throughout the 60-min brain and 180-min whole-body scans (Fig. 8). No evidence of hypoglycemia was seen in any animal following administration of [^{68}Ga]Ga-NOTA-insulin. In fact, there was no significant difference in blood glucose level at any timepoint.

Estimation of human absorbed doses

As the findings from this study will be used to guide future studies of intranasal [^{68}Ga]Ga-NOTA-insulin administration in humans, we used the observed radioactivity uptake to estimate absorbed doses in humans. Final human absorbed doses for both male and female subjects in mSv/MBq were estimated using OLINDA/EXM software (OLINDA 2.2.3) and through the implementation of the recommended guidelines from the International Commission on Radiological Protection (ICRP)-based models (ICRP-89 model),[19,20] The dose estimates for males and females are provided in Table 2.

From the radiation dose estimates in both males and females, the human organ receiving the highest dose would be urinary bladder with 0.128 ± 0.023 mSv/MBq. The next five dose organs and their respective mean dose

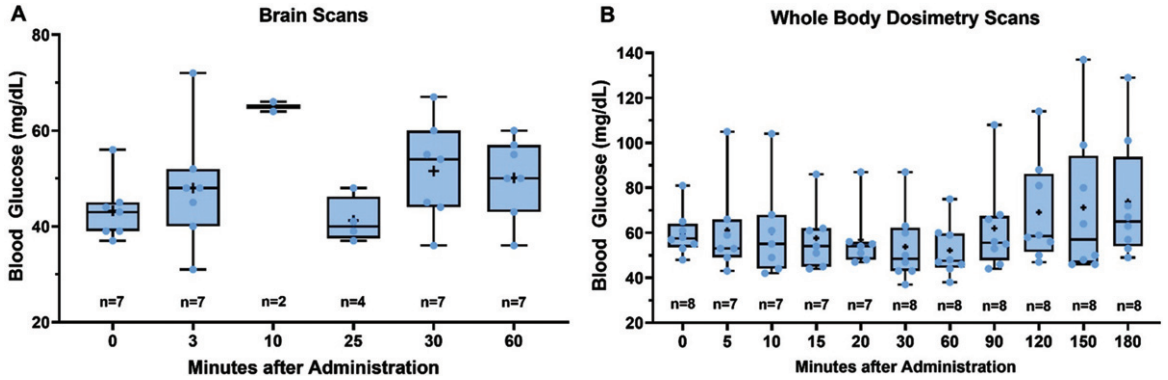

Fig. 8. Blood glucose levels during the A) brain scans and B) whole body dosimetry scans in the time following the intranasal administration of [^{68}Ga]Ga-NOTA-insulin. Black line = median; black+ = mean.

Table 2
Estimated [^{68}Ga]Ga-NOTA-insulin absorbed dose in human males and females, extrapolated from vervet monkey organ distribution data

Organ	Female (mSv/MBq)	Male (mSV/MBq)
Brain	0.0161 ± 0.002	0.0133 ± 0.002
Eyes	0.0568 ± 0.003	0.0353 ± 0.012
Stomach wall	0.1275 ± 0.002	0.1215 ± 0.0451
Colon	0.1327 ± 0.002	0.1057 ± 0.0252
Heart	0.1166 ± 0.0231	0.0934 ± 0.0232
Kidneys	0.0416 ± 0.007	0.0281 ± 0.0068
Liver	0.0266 ± 0.0048	0.0207 ± 0.0054
Lungs	0.0378 ± 0.007	0.0365 ± 0.0221
Pancreas	0.0122 ± 0.0256	0.1043 ± 0.0256
Salivary glands	0.1211 ± 0.0247	0.0972 ± 0.0231
Red marrow	0.0998 ± 0.0191	0.0800 ± 0.011
Spleen	0.0364 ± 0.0074	0.0328 ± 0.0092
Thymus	0.1180 ± 0.0239	0.0951 ± 0.0234
Gallbladder	0.12375 ± 0.00211	0.111 ± 0.0221
Total body	0.1221 ± 0.0244	0.0978 ± 0.0236
Effective dose	$\mathbf{0.0795 \pm 0.011}$	$\mathbf{0.071 \pm 0.028}$

estimates were the stomach (0.124 ± 0.001), colon (0.118 ± 0.0012 mSv/MBq), pancreas (0.116 ± 0.025 mSv/MBq), salivary glands (0.109 ± 0.012 mSv/MBq), and prostate/males (0.107 ± 0.024 mSv/MBq). The mean whole body dose estimate was 0.112 ± 0.024 mSv/MBq and 0.097 ± 0.023 mSv/MBq for males and females, respectively. The mean effective dose (ICRP 89 model) was 0.070 ± 0.011 mSv/MBq. Based on average values, the maximum dose of [^{68}Ga]Ga-NOTA-insulin that can be administered to humans without exceeding the 5 rem (50 mSv)[21] to the urinary bladder is 185 MBq (5.0 mCi), comparable to 15 IU.

DISCUSSION

Dozens of clinical trials investigating INI as a treatment for cognitive decline have revealed effects such as enhanced memory and functional ability, preserved brain volume, and improved AD biomarker profiles. However, the importance of a reliable intranasal delivery device was recently demonstrated in our 18-month phase II trial, where improved cerebral glucose utilization, biomarker profiles, white matter hyperintensity volume progression, and cognition were only observed following INI administration in a cohort of participants that used one of the two delivery devices.[7] With unreliable delivery devices, it becomes difficult to interpret trial outcomes—is a lack of treatment effect due to poor insulin delivery to the brain or failure of insulin to elicit an effect? While the overwhelming success of INI studies suggest the former, it is essential to identify a reliable delivery device that targets insulin to the brain before INI can be used clinically.

A recent study showed successful nose-to-brain delivery of [^{18}F]FB-insulin in rhesus macaque and cynomolgus macaque monkeys.[22] Using dynamic PET imaging, they showed that liquid and aerosolized [^{18}F]FB-insulin, delivered by nasal catheter or tubing, reached with brain within 13 min. In our study, we explored safety and regional localization of a novel PET radiotracer, [^{68}Ga]Ga-NOTA-insulin, following intranasal administration in healthy adult vervet monkeys. To do this, we used the Aptar CPS pump system, after a thorough investigation of intranasal delivery devices revealed confidence in this system to target insulin to the brain. We are hopeful that these findings will help guide future studies of

intranasal [68Ga]Ga-NOTA-insulin administration in humans, where we can further assess the utility of the Aptar CPS intranasal delivery system and other Aptar nasal targeting systems to effectively deliver insulin to the brain.

Specific brain regional activity of [68Ga]Ga-NOTA-insulin

In this study, intranasally administered [68Ga]Ga-NOTA-insulin was clearly delivered to the brain parenchyma and choroid plexus via perivascular channels that circumvented the blood-brain barrier, providing support for the effectiveness of the pump system. We saw uptake of [68Ga]Ga-NOTA-insulin in the brain that lasted for 60 min after intranasal administration, similar to a pattern that has been observed in CD-1 mice following intranasal administration of [125I]-insulin.[23] In the current study, PET imaging allowed for the visualization of [68Ga]Ga-NOTA-insulin in specific brain regions. We found that uptake of the radiolabeled insulin was highest in the amygdala, putamen, choroid plexus, and hypothalamus. Previously, intranasally administered insulin[24] and [125I]-insulin-like growth factor-1 (IGF-1)[25] have been shown to traverse along the olfactory and trigeminal nerves to spread throughout the brain, ultimately ending up in the olfactory bulbs, hippocampus, hypothalamus, cortex, and cerebellum, as shown by the highest qualitative uptake in these regions.[23,26–29] It was unsurprising that we also observed relatively high uptake in the hypothalamus, cortex, hippocampus, and cerebellum in our vervet monkeys. Consistent with our high uptake seen in the putamen, another study of intranasal [125I]-labeled interferon-β1b administration in adult male cynomolgus monkeys showed the strongest signal in the basal ganglia (putamen, globus pallidus, and caudate).[30] In addition, the olfactory nerve is known to project to the amygdala, hippocampus, and parahippocampal regions;[31] therefore, high uptake of [68Ga]Ga-NOTA-insulin in the amygdala and hippocampus provides support that the insulin spread along this pathway to disperse throughout the brain.

It is unsurprising that the highest uptake of insulin occurs in the aforementioned brain regions following intranasal administration, as studies investigating the binding of [125I]-labeled insulin have revealed that insulin receptors are distributed unevenly throughout the brain.[32] In rats, insulin receptors are expressed at the highest density in the olfactory bulb, cerebral cortex, hypothalamus, cerebellum, and choroid plexus.[33–35] Similarly, humans show the highest [125I]-IGF-1 binding density at the hippocampus, amygdala, and parahippocampal gyrus, followed by the cerebellum, cerebral cortex, and caudate nucleus, and then the substantia nigra, red nucleus, white matter, and cerebral peduncles.[36] Insulin can bind to its receptors in these brain regions to elicit downstream effects.

In the investigation of nose-to-brain [18F]FB-insulin, which showed the highest uptake in the limbic and frontotemporal cortical regions, the [18F]FB-insulin reached the brain within 13 min and was highest 27 min after dosing.[22] Our results corroborate these findings, as we demonstrated [68Ga]Ga-NOTA-insulin uptake was high in several brain regions 20–60 min after intranasal administration. Distinctly, our study provides support for the efficacy of the Aptar CPS pump system to target insulin to the brain. We also assessed whole-body dosimetry of [68Ga]Ga-NOTA-insulin to calculate estimated human organ exposure, which is important to understand before [68Ga]Ga-NOTA-insulin can be delivered to humans.

Dosimetry

Biodistribution studies through dosimetry indicate [68Ga]Ga-NOTA-insulin undergoes bowel excretion. Importantly, no organ is exposed to more 2.5 mSv; which is 10-fold lower than the 50 mSv exposure limit set for radiation-sensitive organs. Additionally, vitals remained stable in all vervets during and after the PET scans, and blood glucose levels did not significantly change following intranasal administration of [68Ga]Ga-NOTA-insulin. Together, these results indicate a high safety profile for [68Ga]Ga-NOTA-insulin. It is unsurprising that blood glucose remained relatively stable post administration. Previously, Salameh et al. showed that only 3% of 125I-insulin reached the systemic circulation of male CD-1 mice following intranasal administration.[23] Additionally, several human studies have confirmed that intranasal insulin administration does not lead to hypoglycemia.[37–39]

In our healthy normal nonhuman primate cohort that was scanned, we did not observe any significant differences with regard to age or sex in intranasal [68Ga]-NOTA-insulin uptake in either the brain or dosimetry studies. However, a thorough probing of these relationships is beyond the scope of this study due to the small sample size (i.e., $n = 2$ female brain scans). Overall, the brain and whole-body dosimetry PET scans of [68Ga]-NOTA-insulin in vervets

clearly demonstrate brain penetration and favorable distribution of INI respectively. This preliminary data provides critical information for translating [^{68}Ga]Ga-NOTA-insulin PET with intranasal delivery to humans using the Aptar CPS delivery system. This strategy will create a new paradigm for understanding the intranasal distribution of insulin and advance novel INI-based therapeutic platforms for AD and other neurodegenerative disorders.

Limitations

A limitation of this study is that all vervets were anesthetized during the intranasal administration and intubated during the PET scans. We did our best to recreate the intranasal administration technique that would be employed by an awake human, in that each animal was held in an upright position during the intranasal puffs, and then immediately laid supine for the scan. However, the anesthesia/intubation of the vervets was unavoidable. We did observe some pooling of the [^{68}Ga]Ga-NOTA-insulin in the nasal cavity, which remained for $\sim$60 min following administration, likely a result of the anesthesia. It is our expectation that this pooling will be dramatically decreased in awake humans who can take purposeful sniffs and will be breathing on their own, without a ventilator. It is encouraging that brain uptake was so widespread in these anesthetized vervets; a finding that we believe will be replicated and even improved, with awake human subjects. Additionally, it is possible, albeit unlikely, that the ketamine and isoflurane anesthetization may have interfered with our results. However, we have not come across any conclusive evidence to support this assumption.

Future directions

The results of this study will guide the development of future PET imaging studies following intranasal [^{68}Ga]Ga-NOTA-insulin in human subjects. This will allow for the 1) determination of effectiveness of the Aptar delivery system in delivering [^{68}Ga]Ga-NOTA-insulin to the brain, and 2) visualization of regional biodistribution of [^{68}Ga]Ga-NOTA-insulin. Studies such as these will be essential to move forward with the investigation of INI as a treatment in cognitive decline/AD. Additionally, PET radiotracer quantification with kinetic modeling is needed to assess specific and non-specific radiotracer binding and to capture early changes in biomarkers at disease onset, progression, and treatment. Therefore, our next experiments will be to determine all the critical parameters generated by kinetic modeling of PET data including volume of distribution, binding potential, and maximum binding constants. We will use compartmental modelling with an arterial input function to calculate these parameters.

AUTHOR CONTRIBUTIONS

Kiran Kumar Solingapuram Sai (Conceptualization; Data curation; Formal analysis; Funding acquisition; Investigation; Writing – original draft); Jennifer M. Erichsen (Data curation; Funding acquisition; Investigation; Writing – original draft); Krishna Kumar Gollapelli (Investigation; Writing – review & editing); Ivan Krizan (Investigation; Writing – review & editing); Mack Miller (Data curation; Formal analysis; Writing – review & editing); Avinash Bansode (Writing – review & editing); Matthew J. Jorgensen (Writing – review & editing); Thomas C. Register (Investigation; Writing – review & editing); Charles Cazzola (Writing – review & editing); Reenal Gandhi (Writing – review & editing); Julie Suman (Writing – review & editing); Suzanne Craft (Conceptualization; Funding acquisition; Writing – review & editing).

ACKNOWLEDGMENTS

The authors would like to acknowledge all technicians involved in the care and evaluation of the study animals, especially: Tracy Fairbairn, Chrissy Long, Christie Scott, Justin Herr, and Lori Patterson. The authors also thank the Joseph Bottoms and Freda Crawford, from the Translational Imaging Program (TIP), Wake Forest School of Medicine, for providing instrumental assistance. The authors would like to acknowledge Dr. A.R. Prideaux from Hermes Medical Solution for assistance with dosimetry software analysis.

FUNDING

This work was supported in part by Aptar Pharma, who provided partial funding and the intranasal delivery systems for the study. This work was also supported by the North Carolina Diabetes Research Center Ignition Fund Award Number DK124723.

CONFLICT OF INTEREST

This work was supported in part by Aptar Pharma, who provided partial funding and the intranasal devices for the study, and reviewed the manuscript, but had no input into study design, data analyses, or manuscript preparation.

Jennifer Erichsen is supported by NIA T32 AG033534.

Suzanne Craft is a Scientific Advisory Board member for The Neurodegeneration Consortium.

All other authors have no conflict of interest to report.

DATA AVAILABILITY

The data supporting the findings of this study are available on request from the corresponding author.

REFERENCES

1. van Dyck CH, Swanson CJ, Aisen P, et al. Lecanemab in early Alzheimer's disease. *N Engl J Med* 2022; 388: 9–21.
2. Reardon S. Alzheimer's drug donanemab: what promising trial means for treatments. *Nature* 2023; 617: 232–233.
3. Hoyer S and Nitsch R. Cerebral excess release of neurotransmitter amino acids subsequent to reduced cerebral glucose metabolism in early-onset dementia of Alzheimer type. *J Neural Transm* 1989; 75: 227–232.
4. Yarchoan M and Arnold SE. Repurposing diabetes drugs for brain insulin resistance in Alzheimer disease. *Diabetes* 2014; 63: 2253–2261.
5. Hanson LR and Frey WH, 2nd. Intranasal delivery bypasses the blood-brain barrier to target therapeutic agents to the central nervous system and treat neurodegenerative disease. *BMC Neurosci* 2008; 9 Suppl 3: S5.
6. Lochhead JJ and Thorne RG. Intranasal delivery of biologics to the central nervous system. *Adv Drug Deliv Rev* 2012; 64: 614–628.
7. Craft S, Raman R, Chow TW, et al. Safety, efficacy, and feasibility of intranasal insulin for the treatment of mild cognitive impairment and Alzheimer disease dementia: a randomized clinical trial. *JAMA Neurol* 2020; 77: 1099–1109.
8. Aptar. First Nasally-Administered Pharmaceutical Treatment for Dry Eye Disease Approved by US FDA with Aptar's Nasal Pump System Crytal Lake, IL, 2021.
9. Taubel JC, Nelson NR, Bansal A, et al. Design, synthesis, and preliminary evaluation of [(68)Ga]Ga-NOTA-insulin as a PET probe in an Alzheimer's disease mouse model. *Bioconjug Chem* 2022; 33: 892–906.
10. Harkema JR, Carey SA and Wagner JG. The nose revisited: a brief review of the comparative structure, function, and toxicologic pathology of the nasal epithelium. *Toxicol Pathol* 2006; 34: 252–269.
11. Emami A, Tepper J, Short B, et al. Toxicology evaluation of drugs administered via uncommon routes: intranasal, intraocular, intrathecal/intraspinal, and intra-articular. *Int J Toxicol* 2018; 37: 4–27.
12. Council NR. *Guide for the Care and Use of Laboratory Animals*. 8th ed. Washington, D.C.: The National Academies Press, 2011, p.246.
13. Jasinska AJ, Schmitt CA, Service SK, et al. Systems biology of the vervet monkey. *ILAR J* 2013; 54: 122–143.
14. Frye B, Shively C, Craft S, et al. Co-occurrence of physical and cognitive decline in vervet monkeys (Chlorocebus aethiops sabaeus). *Innov Aging* 2020; 4: 118–118.
15. Marti-Climent JM, Collantes M, Jauregui-Osoro M, et al. Radiation dosimetry and biodistribution in non-human primates of the sodium/iodide PET ligand [(18)F]-tetrafluoroborate. *EJNMMI Res* 2015; 5: 70.
16. Stabin MG, Wendt RE and Flux GD. RADAR guide: standard methods for calculating radiation doses for radiopharmaceuticals, part 2—data analysis and dosimetry. *J Nucl Med* 2022; 63: 485–492.
17. Velikyan I, Rosenström U, Rosestedt M, et al. Improved radiolytic stability of a 68ga-labelled collagelin analogue for the imaging of fibrosis. *Pharmaceuticals* 2021; 14: 990.
18. Gollapelli KK, Damuka N, Bansode A, et al. Preliminary evaluations of [68Ga]-NOTA-insulin in animal models of Alzheimer's disease. *J Nucl Med* 2023; 64: P1228–P1228.
19. ICRP. *Recommendations of the International Commission on Radiological Protection. Annals of the ICRP*. Pergamon Press Oxford, 2008.
20. Valentin J. *The 2007 recommendations of the international commission on radiological protection*. Elsevier, 2008.
21. Devine CE and Mawlawi O. Radiation safety with positron emission tomography and computed tomography. *Semin Ultrasound CT MR* 2010; 31: 39–45.
22. Smith K, Fan J, Marriner GA, et al. Distribution of insulin in primate brain following nose-to-brain transport. *Alzheimers Dement (N Y)* 2024; 10: e12459.
23. Salameh TS, Bullock KM, Hujoel IA, et al. Central nervous system delivery of intranasal insulin: mechanisms of uptake and effects on cognition. *J Alzheimers Dis* 2015; 47: 715–728.
24. Lochhead JJ, Kellohen KL, Ronaldson PT, et al. Distribution of insulin in trigeminal nerve and brain after intranasal administration. *Sci Rep* 2019; 9: 2621. 20190222.
25. Thorne RG, Pronk GJ, Padmanabhan V, et al. Delivery of insulin-like growth factor-I to the rat brain and spinal cord along olfactory and trigeminal pathways following intranasal administration. *Neuroscience* 2004; 127: 481–496.
26. Brabazon F, Wilson CM, Jaiswal S, et al. Intranasal insulin treatment of an experimental model of moderate traumatic brain injury. *J Cereb Blood Flow Metab* 2017; 37: 3203–3218.
27. Renner DB, Svitak AL, Gallus NJ, et al. Intranasal delivery of insulin via the olfactory nerve pathway. *J Pharm Pharmacol* 2012; 64: 1709–1714.
28. Rhea EM, Humann SR, Nirkhe S, et al. Intranasal insulin transport is preserved inaged SAMP8 mice and is altered by albumin and insulin receptor inhibition. *J Alzheimers Dis* 2017; 57: 241–252.
29. Born J, Lange T, Kern W, et al. Sniffing neuropeptides: a transnasal approach to the human brain. *Nat Neurosci* 2002; 5: 514–516.
30. Thorne RG, Hanson LR, Ross TM, et al. Delivery of interferon-beta to the monkey nervous system following intranasal administration. *Neuroscience* 2008; 152: 785–797.

31. Allison AC. The secondary olfactory areas in the human brain. *J Anat* 1954; 88: 481–488.
32. Schulingkamp RJ, Pagano TC, Hung D, et al. Insulin receptors and insulin action in the brain: review and clinical implications. *Neurosci Biobehav Rev* 2000; 24: 855–872.
33. Hill JM, Lesniak MA, Pert CB, et al. Autoradiographic localization of insulin receptors in rat brain: Prominence in olfactory and limbic areas. *Neuroscience* 1986; 17: 1127–1138.
34. Werther GA, Hogg A, Oldfield BJ, et al. Localization and characterization of insulin receptors in rat brain and pituitary gland using *in vitro* autoradiography and computerized densitometry. *Endocrinology* 1987; 121: 1562–1570.
35. Folli F, Ghidella S, Bonfanti L, et al. The early intracellular signaling pathway for the insulin/insulin-like growth factor receptor family in the mammalian central nervous system. *Mol Neurobiol* 1996; 13: 155–183.
36. Adem A, Jossan SS, d'Argy R, et al. Insulin-like growth factor 1 (IGF-1) receptors in the human brain: quantitative autoradiographic localization. *Brain Res* 1989; 503: 299–303.
37. Roque P, Nakadate Y, Sato H, et al. Intranasal administration of 40 and 80 units of insulin does not cause hypoglycemia during cardiac surgery: a randomized controlled trial. *Can J Anaesth* 2021; 68: 991–999.
38. Schmid V, Kullmann S, Gfrörer W, et al. Safety of intranasal human insulin: A review. *Diabetes Obes Metab* 2018; 20: 1563–1577.
39. Craft S, Baker LD, Montine TJ, et al. Intranasal insulin therapy for Alzheimer disease and amnestic mild cognitive impairment: a pilot clinical trial. *Arch Neurol* 2012; 69: 29–38.